

THE LUMINOSITY FUNCTION FOR DIFFERENT MORPHOLOGICAL TYPES IN THE CfA
REDSHIFT SURVEY

RONALD O. MARZKE, MARGARET J. GELLER, AND JOHN P. HUCHRA¹

Harvard-Smithsonian Center for Astrophysics, 60 Garden Street, Cambridge, Massachusetts 02138
Electronic mail: marzke, mjpg, huchra@cfa.harvard.edu

HAROLD G. CORWIN, JR.

California Institute of Technology, IPAC M/S 100-22, Pasadena, California 91125
Electronic mail: hgcjr@ipac.caltech.edu

Received 1993 December 30; revised 1994 March 28

ABSTRACT

We derive the luminosity function for different morphological types in the original CfA Redshift Survey (CfA1) and in the first two slices of the CfA Redshift Survey Extension (CfA2). CfA1 is a complete sample containing 2397 galaxies distributed over 2.7 steradians with $m_z \leq 14.5$. The first two complete slices of CfA2 contain 1862 galaxies distributed over 0.42 steradians with $m_z = 15.5$. The shapes of the E-S0 and spiral luminosity functions (LF) are indistinguishable. We do not confirm the steeply decreasing faint end in the E-S0 luminosity function found by Loveday *et al.* [ApJ, 390, 338 (1992)] for an independent sample in the southern hemisphere. We demonstrate that incomplete classification in deep redshift surveys can lead to underestimates of the faint end of the elliptical luminosity function and could be partially responsible for the difference between the CfA survey and other local field surveys. The faint end of the LF for the Magellanic spirals and irregulars is very steep. The Sm-Im luminosity function is well fit by a Schechter function with $M^* = -18.79$, $\alpha = -1.87$, and $\phi^* = 0.6 \times 10^{-3}$ for $M_z \leq -13$. These galaxies are largely responsible for the excess at the faint end of the general CfA luminosity function [Marzke *et al.* ApJ (in press) (1994)]. The abundance of intrinsically faint, blue galaxies nearby affects the interpretation of deep number counts. The dwarf population increases the expected counts at $B=25$ in a no-evolution, $q_0=0.05$ model by a factor of two over standard no-evolution estimates. These dwarfs change the expected median redshift in deep redshift surveys by less than 10%. Thus the steep Sm-Im LF may contribute to the reconciliation of deep number counts with deep redshift surveys.

1. INTRODUCTION

The origin of galaxy morphology and the relation between morphology and environment are longstanding questions in extragalactic astronomy. Hubble (1926), de Vaucouleurs (1959), and Sandage (1961) pioneered the systematic description of galaxies using classifications determined by eye from photographic plates. Even today, despite rapid advances in automated galaxy detection, types determined by eye remain the preferred measure of galaxy morphology.

Another important discriminant among galaxies is the intrinsic luminosity. Correlations between morphology and luminosity offer insight into the physical processes that drive galaxy formation. The local luminosity function (LF) is thus the starting point for models of galaxy formation and evolution (Dekel & Silk 1986; Schaeffer & Silk 1988; White & Frenk 1991; Lacey *et al.* 1993). Although the similarity among types at the bright end of the LF (Tammann *et al.* 1979) is a stringent test of these models, the faint end of the LF is poorly constrained.

Variation in the LF with galaxy morphology may also

distort the picture of large-scale structure drawn from flux-limited redshift surveys. Reconstruction of the large-scale density field requires accurate knowledge of the LF for each type of galaxy in the survey (Santiago & Strauss 1991). Because of the strong correlation between morphology and local density (Dressler 1980; Postman & Geller 1984), the type-specific LF is particularly relevant when the survey depth is smaller than the coherence length of the structure.

The LF for different types also provides the baseline for studying galaxy evolution. Counts of galaxies as a function of apparent magnitude extend to very faint limits (Koo 1986; Tyson 1988; Metcalfe *et al.* 1991). Interpretation of the number counts depends sensitively on the extrapolation of the faint end of the luminosity function (Koo *et al.* 1993; Tyson 1988; Broadhurst *et al.* 1988). Redshifts for very faint field galaxies are scant, and thus the faint end of the LF is poorly determined even when averaged over all types. The uncertainty in $N(m)$ is exacerbated by K -corrections, which enhance the fractional contribution of intrinsically faint, blue galaxies at high redshift. Thus complete samples of faint galaxies nearby are crucial to our understanding of galaxies in the past.

Detailed studies of the type-specific LF are limited to nearby galaxies, particularly those in the Virgo region (Sandage *et al.* 1985; Binggeli *et al.* 1988, hereafter BST 88). One of the most striking results of the Virgo cluster

¹Visiting Astronomer, Kitt Peak National Observatory, National Optical Astronomy Observatories, NOAO is operated by the Association of Universities for Research in Astronomy, under contract for the National Science Foundation.

survey is the preponderance of dwarf galaxies. Because Virgo galaxies inhabit a dense region of the universe, it is difficult to draw general conclusions about galaxy formation from this sample alone. In addition, some of the criteria for determining cluster membership are related to galaxy morphology (Sandage *et al.* 1985). Without distances or at least redshifts, systematic biases caused by foreground/background contamination are unknown.

The large volume of the CfA redshift survey allows a direct analysis of the type-specific field LF. In Secs. 2 and 3, we describe the data and measure independent LFs for ellipticals, S0's, Sa–Sb's, Sc–Sd's, and Sm–Im's. In Sec. 4.1, we discuss the biases in our sample, and in Sec. 4.2, we compare our results with other field surveys. Section 4.3 addresses the effects of incompleteness in the morphological classification process on the determination of type-specific LFs. In Sec. 4.4, we derive the expected $N(m)$ and $N(z)$ using the LFs derived in Sec. 3 and discuss the implications of the local population of field dwarfs for the study of faint galaxies.

2. DATA

Previous papers contain details of the CfA Redshift Survey data. (Marzke *et al.*, 1993a; Vogeley *et al.* 1992; Huchra *et al.* 1983). Here, we analyze a subsample containing 3933 galaxies with morphological types. The sample consists of all galaxies in the first two slices of CfA2 ($8^{\text{h}} \leq \alpha \leq 17^{\text{h}}$, $26.5^{\circ} \leq \delta \leq 38.5^{\circ}$) and all galaxies in CfA1 not included in CfA2. Burg (1987) and Efstathiou *et al.* (1988) have partially analyzed CfA1.

Apparent magnitudes are from the Zwicky catalog. Because of uncertainties in the transformations, we do not transform the magnitudes to other systems (Marzke *et al.* 1993a). We use the reddening maps of Burstein & Heiles (1982) and a standard extinction law $A_B = 4.0E(B - V)$ to correct apparent magnitudes for extinction in the Galaxy. We correct both the apparent magnitude and the magnitude limit at each galaxy position. We also correct the apparent magnitudes for K -dimming using the type-dependent corrections derived by Pence (1976) and used in the RC2:

$$\Delta m = K'_B(T)cz,$$

$$10^4 K'_B(T) = \begin{cases} 0.15, & T \leq 0; \\ 0.15 - 0.025T, & 0 \leq T \leq 3; \\ 0.075 - 0.010(T - 3), & T \geq 3. \end{cases}$$

Because of the uncertainty in the dependence of galaxy brightness on viewing angle (Burstein *et al.* 1991; Valentijn 1990; Lauberts & Valentijn 1989; Disney *et al.* 1989), we do not correct for internal extinction. Galaxy distances are calculated directly from their redshifts in the Local Group frame: $v_{\text{corr}} = v_{\odot} + 300 \sin l \cos b$. We assume $H_0 = 100 \text{ km s}^{-1} \text{ Mpc}^{-1}$. Section 3 includes a discussion of the effects of Virgo infall.

For the galaxies in CfA2, H.G.C. assigned morphological types by eye using copy plates from the first Palomar Sky Survey. J.P.H. assigned types using the KPNO POSS for all galaxies without types from the Second Reference Catalogue (de Vaucouleurs *et al.* 1976) or from the UGC (Nilson 1973).

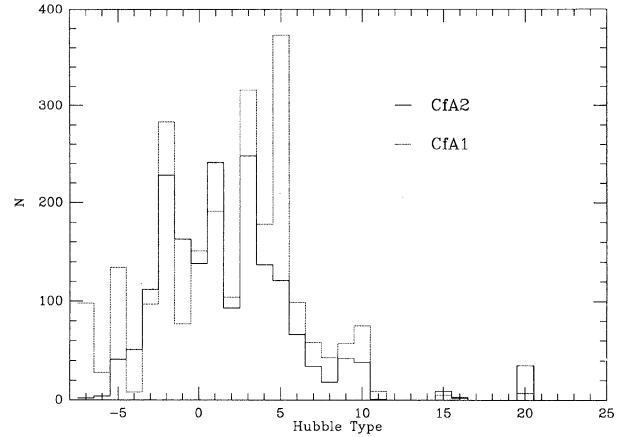


FIG. 1. Distribution of Hubble types in CfA1+2. Dotted line is for CfA1, solid line is for CfA2.

The typing is thus more homogeneous in CfA2 than in CfA1. The types in CfA2 are accurate to approximately $\pm 1T$.

We divide the samples into five type bins: ellipticals ($-7 \leq T \leq -4$), S0's ($-3 \leq T \leq 0$), Sa–Sb ($1 \leq T \leq 4$), Sc–Sd ($5 \leq T \leq 7$), and Sm–Im ($8 \leq T \leq 10$). A small number of galaxies in this sample could only be classified as spiral but not subtyped; these are in bin $T = 20$ ($\sim 1\%$ of the sample). Fourteen galaxies could not be classified at all, and are listed as $T = 15$.

Figure 1 shows the distribution of raw Hubble types in CfA1 and CfA2. These distributions differ because they sample different structures; the morphological mix varies with local density (Dressler 1980; Postman & Geller 1984). CfA1 galaxies also have generally larger diameters and therefore usually have a larger number of resolution elements. This generally leads to later classifications for spirals, which may contribute to the excess of late-type ($T \geq 2$) galaxies in CfA1. Although this bias is probably small compared to the bias introduced by the morphology–density relation, it could play a role in shaping the type-specific LFs. This effect is discussed further in Sec. 4.1.

3. RESULTS

Figure 2 shows the type-dependent LFs for CfA1 and for CfA2. We derive these LFs using the stepwise maximum likelihood method (SWML) of Efstathiou *et al.* (1988). Except for the early spirals, CfA1 and CfA2 are consistent. The ratio of bright/faint Sa–Sb galaxies in CfA1 is larger than in CfA2. This discrepancy is not caused by large-scale flows or by population differences in the Virgo Cluster. Figure 3 shows the Sa/Sb LF corrected for Virgo infall and with Virgo galaxies removed. The forms of the individual LFs change, but the discrepancy between CfA1 and CfA2 remains. We discuss this discrepancy further in Sec. 4.

Because CfA1 and CfA2 are broadly consistent, we combine the samples for further analysis. Figure 4 shows SWML LFs for each type in the Combined sample. Although Virgo

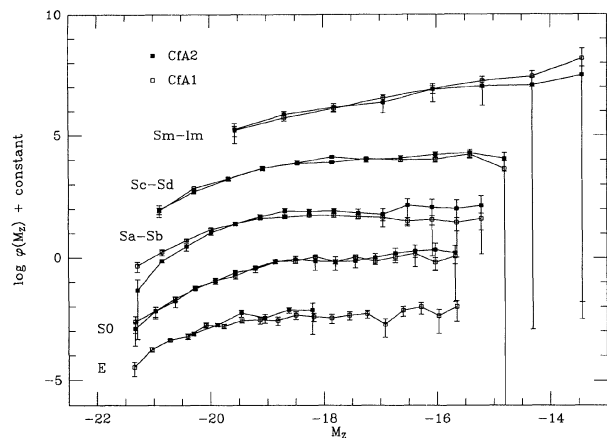


FIG. 2. Comparison of SWML LFs for different morphological types in CFA1 (open squares) and in CFA2 (filled squares).

infall affects the shape of the LFs, the effect is small, and the LF of each type relative to the total LF changes insignificantly when Virgo infall is included.

Table 1 lists Schechter function parameters for the type-specific LFs. The fits include all galaxies fainter than $M_Z = -21.5$. The E, Sa–Sb, and Sm–Im LFs are well described by Schechter functions, as shown by the likelihood ratio test in column 4 of Table 1. A high value of $P(\mathcal{L}_1/\mathcal{L}_2)$ indicates that the Schechter fit is not rejected. Although the Schechter fits to the S0 and Scd LFs are not particularly good, they are not strongly rejected, and provide good overall estimates of the shapes of the LFs. Figure 5 shows 1σ confidence intervals for each type. At the faint end, none of the SWML estimates deviate systematically from the Schechter fits. We calculate the normalization ϕ^* (column 5 of Table 1) using the near minimum-variance estimator of the mean density $n_1 = (1/V)\sum_i [1/\psi(r_i)]$, where ψ is the selection function and the sum is over all galaxies with

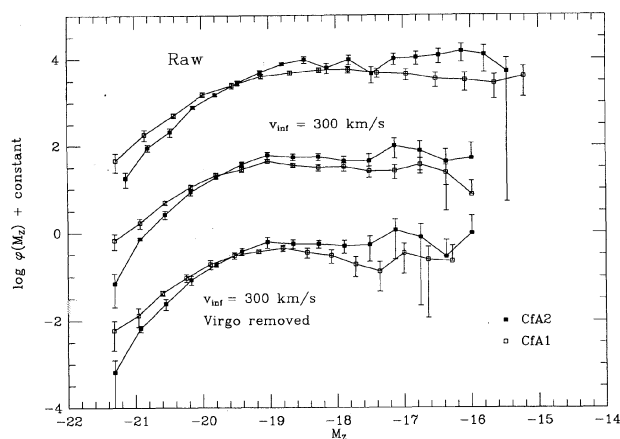


FIG. 3. Comparison of Sa–Sb LFs derived from CFA1 (open squares) and from CFA2 (filled squares). In the top LF, velocities are corrected to Local Group frame; middle LF is corrected for 300 km/s Virgo infall; bottom LF is corrected for 300 km/s Virgo infall, and all galaxies within 20° of M87 are removed.

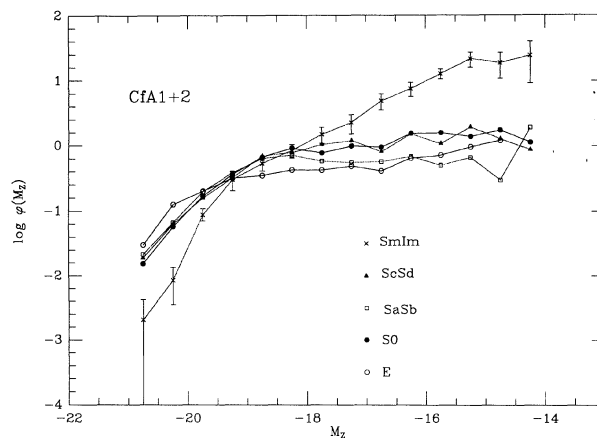


FIG. 4. LFs for different morphological types derived from the combined sample CFA1+2. Error bars are for the smallest sample (Sm–Im); others are omitted for clarity.

$500 \leq cz \leq 12\,000 \text{ km s}^{-1}$ (Yahil *et al.* 1991; Davis & Huchra 1982). The uncertainty in ϕ^* is dominated by large density fluctuations on the scale of the survey. We estimate this uncertainty by calculating the mean density in radial shells and measuring the rms deviation of each shell from the mean density.

Figure 6 shows the normalized Schechter function fits for all types. The uncertainty in ϕ^* dominates the uncertainty in the density at each magnitude (Marzke *et al.* 1993a). Because the majority of Sm–Im's are faint, they are only visible nearby; thus the normalization is particularly sensitive to large-scale structure. Though the normalizations remain uncertain, Fig. 6 indicates that the Sm–Im's dominate the faint end of the general LF. The dwarf LF overtakes the spiral and S0 LFs roughly between -15 and -16 , depending sensitively on errors in the normalization. We can check that the type fractions are consistent by comparing the sum of the type-specific LFs with the SWML estimate of the sample as a whole. There is no significant difference between these estimates, indicating that our normalizations are self-consistent.

Figure 7 shows the combined E–S0 LF and the combined spiral (Sa–Sd) LF. These LFs are indistinguishable. The E–S0 LF is well fit by a Schechter function with $M^* = -18.87$, $\alpha = -0.92$, and $\phi^* = 1.0 \times 10^{-2} \text{ Mpc}^{-3}$. The Schechter parameters for the spiral LF are $M^* = -18.76$, $\alpha = -0.81$ and $\phi^* = 1.5 \times 10^{-2} \text{ Mpc}^{-3}$.

TABLE 1. Schechter function fits.

Sample	M^*	α	$P(\ln \mathcal{L}_1/\mathcal{L}_2)$	$\phi^* (\times 10^{-3} \text{ Mpc}^{-3})$
Elliptical	-19.23	-0.85	0.72	1.5 ± 0.4
S0	-18.74	-0.94	0.10	7.6 ± 2.0
Sa–Sb	-18.72	-0.58	0.55	8.7 ± 2.2
Sc–Sd	-18.81	-0.96	0.04	4.4 ± 1.1
Sm–Im	-18.79	-1.87	0.46	0.6 ± 0.2
All	-18.90	-1.02	0.25	20.1 ± 5.0

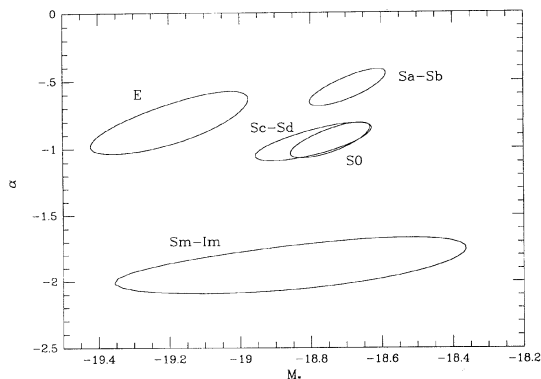


FIG. 5. 1σ confidence intervals for Schechter function fits to the combined sample CfA1+2.

4. DISCUSSION

4.1 Systematic Errors in the Zwicky LF

The differences among type-specific LFs cannot all be ascribed to random errors. In this section, we attempt to distinguish physical differences from artifacts caused by systematic errors. The dominant systematic errors arise from the magnitude scale and from the assignment of morphological types. The results of the previous section beg the following questions: (1) are the early and late spiral LFs significantly different? (2) are ellipticals significantly brighter than S0's and spirals? (3) is the steep slope of the Sm-Im LF real?

The ratio of late to early-type spirals appears to increase toward faint magnitudes. If this behavior is an artifact, the most likely source of error is the typing process itself. Fainter Sa's are difficult to distinguish from S0's. Because of the subtlety of the spiral structure, Sa's are mistaken for S0's more often than the other way around. If we lump the transition class S0/a with the early spirals rather than with the S0's, the difference between early and late types is much less significant. Thus, we regard this difference as an artifact.

For ellipticals, the value of M^* is brighter than for other

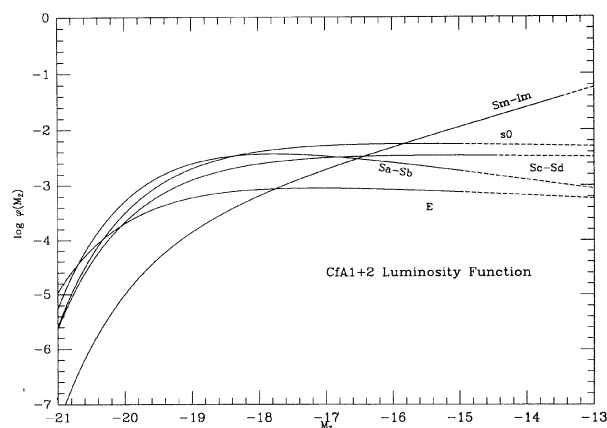


FIG. 6. Schechter function fits to the combined sample CfA1+2. Solid lines indicate the range over which we fit the data; dotted lines indicate extrapolation.

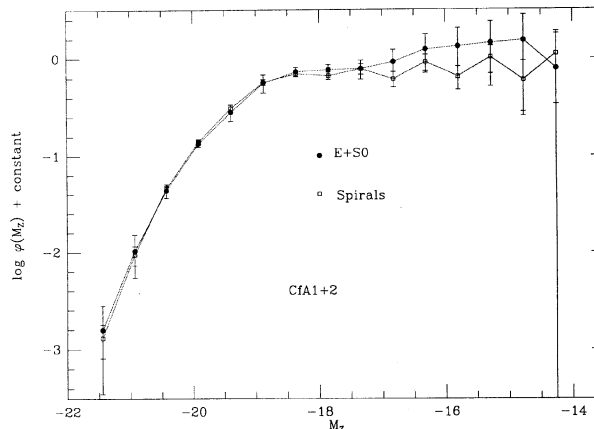


FIG. 7. LFs for the combined spirals and for the combined E+S0 samples.

types (see Table 1). This discrepancy may be a surface-brightness effect. Auman *et al.* (1986), de Vaucouleurs *et al.* (1991:RC3), and Ichikawa & Fukugita (1992) demonstrate that the Zwicky scale depends on surface brightness. The level of this dependence is unclear; the number of Zwicky galaxies with accurate surface photometry is small. However, the trend is that the luminosities of compact galaxies tend to be overestimated. Ichikawa & Fukugita (1992) claim that the Zwicky magnitudes for galaxies smaller than an arcminute are too bright by almost half a magnitude. This bias might explain the unusually bright M^* for the ellipticals. On the other hand, such a bias would make the ellipticals in CfA1 appear significantly fainter than those in CfA2; we observe only a suggestive trend in the opposite direction. Unfortunately, the number of ellipticals in CfA2 is small, and they are almost all distant and therefore intrinsically bright. Thus the faint end of the CfA2 LF is completely undetermined. CfA1, however, contains 268 ellipticals which are well distributed in absolute magnitude. The value of M^* derived from CfA1 is -19.44 without Virgo infall, -19.48 with Virgo infall, and -19.32 with infall but with Virgo galaxies excluded. The corresponding values for CfA12 are -19.23 , -19.39 , and -18.99 . Because α varies among these sub-samples and because M^* and α are correlated, this test is not very restrictive. If anything, the galaxies between 14.5 and 15.5 in CfA2 are too faint, contradicting the results of Ichikawa & Fukugita (1992). Because the surface-brightness effects remain unresolved, the significance of the difference between ellipticals and the rest of the sample is unclear.

The faint end of the Sm-Im LF is substantially steeper than for all other types. Though the number of galaxies in the individual sample is small, the individual LFs for CfA1 and CfA2 are consistent. The faint end slope of the Sm-Im's is steeper than the general LF by more than 3σ . An inordinately large-scale error would be required to explain this difference. We conclude that the LFs for E's all the way through late spirals are broadly consistent; the Sm-Im's constitute a separate population with a distinct luminosity function.

4.2 Comparison with Previous Results

Burg (1987) calculates type-dependent LF's for CfA1 using the binned least-squares technique (Felten 1977; Huchra

1977). Although we have chosen a slightly different type binning, our results are consistent with Burg (1987). In particular, he notes the steep faint end for the Sm–Im class. The discrepancies at the bright end among different types are smaller in our analysis than in his. We attribute this difference to our use of an inhomogeneity-independent technique.

The value of M^* derived from the entire CfA2 sample (Marzke *et al.* 1993) is significantly fainter than the value determined from other field surveys (Efstathiou *et al.* 1988; Loveday *et al.* 1992). This discrepancy is reflected in the type-specific LFs. Because the source of this discrepancy is unknown, we compare only the shapes of the LFs, which are largely determined by the faint end slopes. If scale errors among catalogs are small, the relative proportions of faint and bright galaxies are preserved even when the zero-points differ significantly.

BST88 derive type-specific LFs for the Virgo cluster and for the local field. They emphasize that the field sample is small; for some types, fewer than ten galaxies determine the LF. Because the BST 88 distributions are heavily smoothed, we cannot compare the LFs directly. We find no evidence for a precipitous decline at the faint end in either the elliptical or the S0 LF; a steep falloff is plainly evident in the BST88 field sample for these types. However, we do not separate dwarf ellipticals from giant ellipticals; if the dwarf and giant elliptical LFs in BST88 are combined, their early-type LF is consistent with ours. Our results for the Sm–ImS are also roughly consistent with BST88, although our data do not allow detection of a turnover at $M_{B_T} \geq -13.5$.

Efstathiou *et al.* (1988) derive LFs for E–S0's and spirals in the Anglo-Australian Redshift Survey (AARS). While the faint end slope for early types in the AARS is -0.48 , the error is large, and their result is consistent with ours. They also rederive the LF for different types in the RSA (Sandage & Tammann 1981) and in the sample of Kirshner *et al.* (1979). Although the type binning is different and the RSA errors are large, the RSA faint-end slopes are consistent with the slopes measured from CfA1+2. The faint-end slopes from the Kirshner *et al.* sample are steeper than ours, but the difference is smaller than 2σ .

Metcalfe *et al.* (1991) give Schechter function parameters for a sample of 279 galaxies divided into three color regimes. Although their sample is small, their accurate, multicolor CCD photometry allows one of the better determinations of the local field LF. Because the dispersion in color for a given Hubble type is large, the comparison of type-dependent LF's with color-dependent LF's is not straightforward. However, if we use the conversion between $B-V$ and morphological type applied by Metcalfe *et al.* (1991), our results are consistent with theirs. Their early type LF rolls off slightly faster toward the faint end than ours, but the results are within 2σ .

Loveday *et al.* (1992) compute LFs for 311 early types (E–S0) and 999 spirals using the Stromlo-APM Redshift Survey. They find a flat faint end for spirals, consistent with our results. Their elliptical LF, however, declines steeply at the faint end. The difference in the Schechter faint-end slope between CfA early types and Stromlo-APM early types is striking: $\alpha_{\text{APM}} = +0.2$, $\alpha_{\text{CfA}} = -0.9$. Loveday *et al.* (1992) note, however, that the sample of early types is incomplete at

high redshift. We suggest in the next section that this incompleteness could contribute to the discrepancy between our early-type LF and the one derived from the Stromlo-APM survey.

4.3 Systematic Bias in Type-Specific Luminosity Functions

The quality of a morphological classification depends on the number of resolution elements in the galaxy image. The resolution on a modern, fine-grained photographic plate is limited by the seeing; thus the number of resolution elements per galaxy depends on the seeing and on the galaxy's distance and surface-brightness profile. Because magnitude-limited catalogs sample a broad range in distance and absolute size, the quality of the morphological types is not uniform. Systematic errors arise if the apparent size (and thus the quality of the type) is correlated with the absolute luminosity of the galaxy.

Using photographic surface photometry of Virgo ellipticals, Binggeli *et al.* (1984, hereafter referred to as BST84) find a correlation between the effective radius and the total absolute magnitude for elliptical galaxies. The slope of this correlation changes at $M \sim -18.5$, suggesting that elliptical galaxies separate into two distinct populations (Wirth & Gallagher 1984; Kormendy 1985). The range of surface brightness at faint absolute magnitude is uncertain and is subject to systematic biases. For example, the field abundance of high surface-brightness dwarfs like M32 is unknown, although large-scale plate surveys suggest that they are rare (Binggeli *et al.* 1990).

We use the mean correlation between size and magnitude from BST84 to determine the distribution of apparent isophotal areas in a simulated magnitude-limited sample of elliptical galaxies (cf. Ferguson 1992). We assume that ellipticals follow deVaucouleurs-law surface-brightness profiles (deVaucouleurs 1948), which are completely specified by the absolute magnitude and the effective radius. Although the surface-brightness profiles of galaxies fainter than $M_{B_T} = -16.5$ are more diffuse than a deVaucouleurs law (BST84), few such galaxies exist in magnitude-limited samples, and these galaxies do not significantly affect our analysis. We begin with Monte Carlo simulations of uniform galaxy distributions with Schechter luminosity functions. We remove galaxies fainter than the selected magnitude limit, and then assign effective radii to the remaining galaxies using the mean relation from BST84:

$$\log r_e \approx \begin{cases} -0.3M_{B_T} - 2.4, & M_{B_T} \leq -18.5; \\ -0.1M_{B_T} + 1.4, & M_{B_T} \geq -18.5, \end{cases}$$

where r_e is in parsecs. This expression is adjusted to $H_0 = 100 \text{ km s}^{-1} \text{ Mpc}^{-1}$, and we assume Gaussian scatter about the mean relation to approximate Fig. 7 of BST84. We ignore the contribution of high surface-brightness dwarfs like M32. For a deVaucouleurs profile, the surface brightness at the effective radius is

$$\mu_e = M + 5 \log r_e + 24.96,$$

where μ_e is in magnitudes arcsecond $^{-2}$. We assume the galaxy image is circular, and calculate the area using the 25

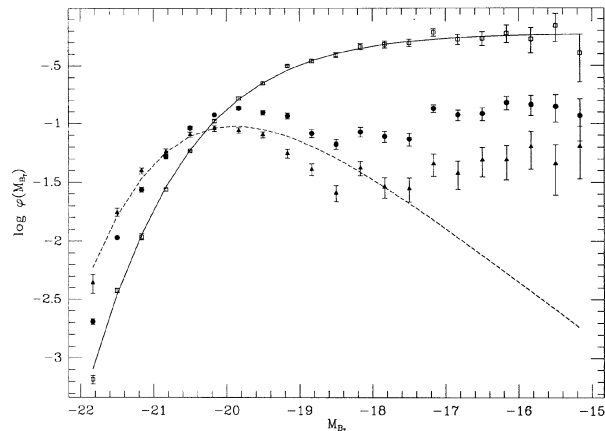


FIG. 8. Effect of resolution limits in galaxy classification on the type-specific LF. Open squares (solid line) are the original LF calculated from Monte Carlo simulations of a magnitude-limited sample with $m_{\text{lim}}=17$. The LF for the simulation is the general LF from Loveday *et al.* (1992). Filled circles represent the LF derived from a resolution-limited subsample of the simulation assuming a deVaucouleurs-law surface-brightness profile, a classification limit of 100 resolution elements and 2'' seeing. Filled triangles represent 2.5'' seeing. The dotted line is the early-type LF derived by Loveday *et al.* (1992).

mag arcsec⁻² isophote. We also assume the limit $z \ll 1$. From Kent (1985),

$$r_{25} = r_e \left[1 + \frac{25 - \mu_e}{8.325} \right]^4.$$

The number of resolution elements is approximately

$$N_{\text{res}} \approx 0.04 \left(\frac{H_0 r_{25}}{cz s} \right)^2,$$

where s is the seeing in arcseconds.

Galaxy classifications are suspect when the number of resolution elements drops below ~ 100 . This limit imposes an effective *diameter* limit on the sample of classified galaxies; this classified sample may not fairly represent the *magnitude*-limited sample as a whole. To model this effect, we assume that the average resolution during a photographic plate survey is 2'' (appropriate for the POSS I plates) and remove all galaxies with fewer than 100 resolution elements. We use a magnitude limit $B_T=17$ and we assume that the true early-type LF is the same as the general LF from the Stromlo-APM survey. Figure 8 shows the LFs calculated from resolution-limited subsamples of the Monte Carlo simulation. To illustrate the dependence on the seeing, we also show the results of a resolution-limited sample compiled in 2.5'' seeing. The effect is quite dramatic. As expected, fainter galaxies are absent from the resolution-limited LF. Table 2 gives Schechter parameters and V/V_{max} for the resolution-limited samples. For comparison, Table 2 includes Schechter parameters for early types from the Stromlo-APM survey. The resolution-limited V/V_{max} is similar to the Stromlo-APM value for the case of 2'' seeing. The dotted line in Fig. 8 shows the Stromlo-APM LF for early-type galaxies. The resolution limit culls distant ellipticals preferentially, and causes an underestimate of the abundance of faint gal-

TABLE 2. Monte Carlo simulations of early-type galaxies.

Seeing	N	M^*	α	V/V_{max}
0''	10000	-19.48	-0.97	0.50
2''	4740	-19.76	-0.37	0.33
2.5''	2742	-19.98	-0.15	0.22
Stromlo-APM	311	-19.84	+0.20	0.32

axies. Because the resolution limit is most effective just fainter than M^* , the most heavily weighted range in the Schechter function fit, the faint-end slope α provides a particularly poor description of the LF for $M_{B_T} \geq -18$.

We have similarly analyzed spiral galaxies using a combined deVaucouleurs law and exponential disk for the surface-brightness profile. Because of the disk, the average spiral galaxy is bigger than the average elliptical of the same apparent magnitude. Thus the effects of the resolution limit are much less drastic. Bulge-dominated S0 galaxies lie somewhere in between. Because of the wide range of bulge-to-disk ratio, internal absorption, spiral structure, and H II region populations in spirals, the simple isophote analysis is naive, and we do not present the results here. Instead, we illustrate the effect by imposing a photographic area limit on a magnitude-limited sample of real galaxies. All galaxies in CfA1 have major and minor-axis diameters taken from Nilsson (1973) or measured by J.P.H.. Figure 9 shows the LF measured from various area-limited subsamples of CfA1. It is clear from the LFs that ellipticals are much more sensitive than the spirals to resolution limits in the classification process.

Figures 8 and 9 show that the resolution limit produces LFs that are qualitatively similar to the early-type LF found by Loveday *et al.* (1992). It is unlikely, however, that this effect explains all of the discrepancy in the early types between the Stromlo-APM and the CfA surveys. For example, the resolution limit is much less effective for S0's, which are lumped into the Stromlo-APM early-type LF. The results of this section simply demonstrate that magnitude-limited samples complete with types for all galaxies are critical for

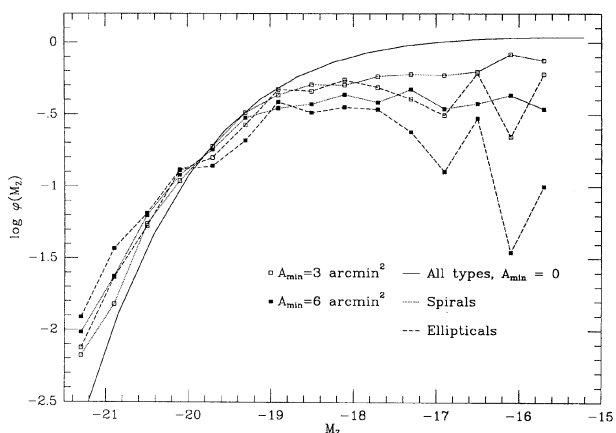


FIG. 9. Effect of photographic area limit on LFs for early and late types in CfA1.

the determination of accurate LFs for different morphological types.

4.4 Implications for Deep Counts

Direct determination of the faint end of the LF is crucial for predicting faint galaxy counts. Most magnitude-limited surveys only hint at the faint end of the LF because the majority of the sample galaxies lie near M^* regardless of the magnitude limit. The most common practice is to extrapolate the Schechter function to faint absolute magnitudes (Tyson 1988; Metcalfe *et al.* 1991, etc.). Unfortunately, the faint-end slope of the Schechter function is determined largely by bright galaxies and may have little to do with the behavior of the LF for $M \geq -16$. Here, we observe the faint end directly. In this section, we discuss the implications of our results, particularly the steep Sm–Im LF, for deep galaxy counts.

Standard models for deep galaxy counts are based on LFs with relatively flat faint ends (Tyson 1988; Broadhurst *et al.* 1988). If the luminosity function does not evolve, the galaxy counts at $B=25$ exceed these predictions by a factor of 5–15, depending on Ω and on the particular choice of LF (cf. Koo & Kron 1992). This was originally interpreted as evidence for strong evolution in galaxy luminosities (e.g., Tyson 1988). On the other hand, deep redshift surveys turn up few galaxies at $z \geq 1$, where many would be expected in the case of strong luminosity evolution (Broadhurst *et al.* 1988; Colless *et al.* 1990; Koo & Kron 1992; Cowie *et al.* 1991). This apparent paradox opened the door for many alternative explanations of the faint blue galaxies, including frequent galaxy mergers, bursting populations of dwarfs, and a nonzero cosmological constant (cf. Cowie *et al.* 1991; Broadhurst *et al.* 1992; Fukugita *et al.* 1990).

The redshift distribution of galaxies fainter than $B \sim 23$ is poorly known (for a review, see Koo & Kron 1992). Many investigators argue that the majority of these faint galaxies lie at high redshift. For example, Tyson (1988) argues that the colors of the galaxies alone distinguish the galaxies at $m \geq 20$ from local DDO and UGC dwarfs; in particular, the $R-I$ colors of the faint galaxies are much redder than those of the known local dwarfs. A stronger argument against a large population of nearby dwarfs comes from symmetric distortions of the faint galaxies in the direction of rich clusters. Tyson *et al.* (1990) attribute these distortions to gravitational lensing of a background population by the foreground cluster potential. They calculate that 70% of the galaxies with $m > 22$ must have redshifts larger than 0.9.

Deep pencil-beam redshift surveys provide direct constraints on the local dwarf population. Broadhurst *et al.* (1988) find that the nearby redshift distribution is incompatible with several *ad hoc* models that include faint dwarf populations. It is interesting to see how the LF derived in this paper affects the expected counts and redshift distributions at faint apparent magnitudes. Using K -corrections from Metcalfe *et al.* (1991) and assuming no evolution and $q_0=0.05$, we find that the expected median redshift in a deep pencil beam survey to $B \sim 21$ changes by less than 10% when the faint dwarfs are included. On the other hand, the dwarfs increase the expected counts at $B=25$ by a factor of two. Thus

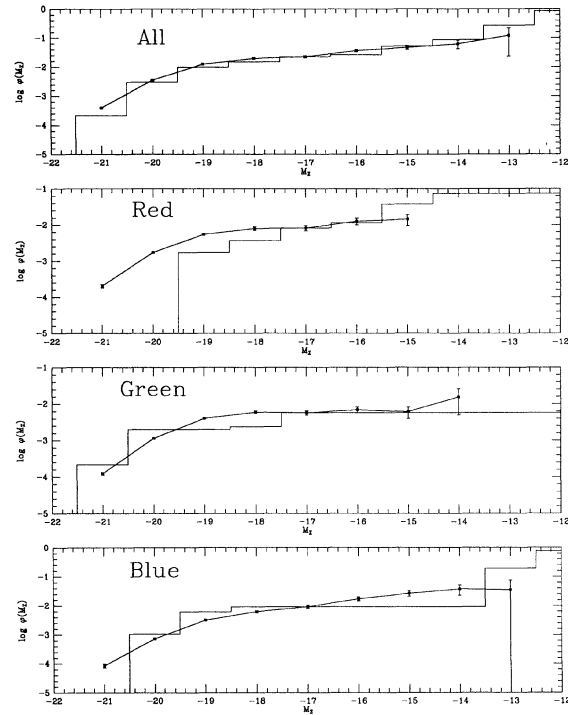


FIG. 10. Comparison of LFs derived by Koo *et al.* (1993) with color-dependent LFs in CfA1+2. Colors for CfA1+2 galaxies are inferred from morphology using the rough transformation in Metcalfe *et al.* (1991).

the dwarfs reduce the discrepancy between the observed counts and the predictions of no-evolution models, but they cannot account for the excess entirely.

Koo *et al.* (1993, KGB) attempt to reproduce the observed counts, colors, and deep redshift distributions by adjusting the luminosity functions for galaxies of different color. Applying Bruzual's models for passive galaxy evolution (Bruzual & Charlot 1993), they find that the predicted counts in B and K as well as the predicted redshift distributions are much closer to the observations if (1) Ω is low and (2) the faint end of the general LF is steep. They argue that the remaining discrepancies (approximately a factor of two in the B counts) are small and may be explained by mild luminosity evolution. Figure 10 shows a comparison between their predicted B_j LF and our general LF averaged over all types. The agreement is striking.

If we break down the LF by color, however, our agreement with KGB is not so good. Because the distribution of color for each Hubble type is broad (deVaucouleurs 1977; Huchra 1977; Marzke *et al.* 1993b), the transformation between morphological type and color is not straightforward. Nevertheless, we can divide our sample into type bins which approximate *on average* the color bins in KGB. We use types $-7:0$ for $B-V \geq 0.85$, $1:4$ for $0.6 \leq B-V \leq 0.85$, and $5:10$ for $B-V \leq 0.6$. We label these samples Red, Green, and Blue, respectively. This choice of bins is rather generous to the Red sample; many S0's are bluer than $B-V=0.85$. Figure 10 shows the LFs for Red, Green, and Blue with the LFs predicted in KGB. Because the normalizations of the CfA

LF's are uncertain, we normalize to KGB for each sample individually at $M = -17$ to compare the shapes.

None of the color-specific KGB LFs fit the observations well. One could argue that the Blue and Green LFs are reasonably close, and that a more suitable color/type transformation would improve the fit. In addition, the magnitude transformation between B_J and m_Z is not well known. The Red sample, however, is strongly rejected by the data. The dearth of bright red galaxies in the KGB LF is evident in their comparison to Metcalfe *et al.* (1991) and is also reflected here. Because the binning error probably *adds* galaxies artificially to the Red sample, it is unlikely that this disparity is caused by an inappropriate color/type transformation.

While the details of the LF predicted by KGB are still in question, the steep faint end of the general LF in KGB is supported by our data. Thus the abundance of faint galaxies nearby may contribute to a reconciliation of deep redshift data with deep number counts.

5. CONCLUSIONS

The luminosity functions for E-S0 and spiral galaxies are indistinguishable in the CfA survey. We find small differences between E and S0 and between early- and late-type spirals, but these differences may be caused by systematic errors in the catalog. The Sm-Im LF is very steep at the faint end, and is well fit by a Schechter function with $M^* = -18.79$, $\alpha = -1.87$, and $\phi^* = 0.6 \times 10^{-3}$. These galaxies contribute most of the faint end excess in the general luminosity function.

We demonstrate that earlier determinations of type-dependent LFs from deeper samples are subject to a classi-

fication bias. Because the classification of a galaxy is linked to its absolute magnitude through a correlation between absolute size and brightness, the LF derived from samples with incomplete types underestimates the abundance of ellipticals fainter than M^* . This incompleteness is reflected in a low value of V/V_{\max} for ellipticals. This bias could partially explain the lack of faint early-type galaxies in deeper surveys such as Loveday *et al.* (1992).

The Sm-Im LF increases the expected counts at $B=25$ by a factor of two without changing the expected median redshift at $B \sim 21$ by more than $\sim 10\%$. Thus the abundance of dwarf galaxies nearby may contribute to the reconciliation of deep number counts with deep redshift surveys. The general LF is consistent with the predictions of Koo *et al.* (1993), but the red end of the KGB LF is deficient in bright galaxies, consistent with Metcalfe *et al.* (1991). Because of the difficulty in inferring color from morphological type alone, we plan to obtain colors for all of the intrinsically faint galaxies in our sample. In addition, we have compiled a magnitude-limited subsample from the ESO catalog to test color-dependent LFs directly (Marzke *et al.* 1993b). With these multicolor samples of apparently bright galaxies, we hope to constrain the relative populations of faint galaxies nearby in order to improve our understanding of galaxies in the past.

We thank Luiz daCosta, Michael Kurtz, Caryl Gronwall, and David Koo for helpful discussions and comments. We also thank the anonymous referees for careful readings of the manuscript and for useful suggestions. R.M. is supported by NASA Grant No. NGT-50819. J.P.H. is partially supported by NASA *HST* Grant No. GO-2684.08-87A. This research is supported in part by NASA Grant No. NAGW-201 and by the Smithsonian Institution.

REFERENCES

- Auman, J., Fahlman, G., & Hickson, P. 1986, *PASP*, 98, 1213
 Binggeli, B., Tarengi, M., & Sandage, A. 1990, *A&A*, 228, 42
 Binggeli, B., Sandage, A., & Tarengi, M. 1984, *AJ*, 90, 1681 (BST84)
 Binggeli, B., Sandage, A., & Tammann, G. A. 1985, *AJ*, 90, 1759
 Binggeli, B., Sandage, A., & Tammann, G. A. 1988, *ARA&A*, 26, 509 (BST88)
 Binggeli, B., Tarengi, M., & Sandage, A. 1990, *A&A*, 228, 42
 Bothun, G. D., & Cornell, M. E. 1990, *AJ*, 99, 1004
 Broadhurst, T. J., Ellis, R. S., & Glazebrook, K. 1992, *Nature*, 355, 55
 Broadhurst, T. J., Ellis, R. S., & Shanks, T. 1988, *MNRAS*, 235, 827
 Burg, R. I. 1987, Ph.D. thesis, Massachusetts Institute of Technology
 Bruzual, A. G., & Charlot, S. 1993, *ApJ*, 405, 538
 Burstein, D., & Heiles, C. 1982, *AJ*, 87, 1165
 Burstein, D., Haynes, M. P., & Faber, S. M. 1991, *Nature*, 353, 515
 Colless, M., Ellis, R. S., Taylor, K., & Hook, R. N. 1990, *MNRAS*, 205, 1287
 Cowie, L. L., Songaila, A., & Hu, E. M. 1991, *Nature*, 354, 460
 Davis, M., & Huchra, J. P. 1982, *ApJ*, 254, 437
 Dekel, A., & Silk, J. 1986, *ApJ*, 303, 39
 de Vaucouleurs, G. 1948, *Ann. d'Astrophys.*, 11, 247
 de Vaucouleurs, G. 1959, *Handbuch der Physik* (Springer, Berlin), pp. 53, 275
 de Vaucouleurs, G. 1977, in *The Evolution of Galaxies and Stellar Populations*, edited by B. M. Tinsley and R. B. Larson (Yale University Observatory, New Haven)
 de Vaucouleurs, G., de Vaucouleurs, A., & Corwin, Jr. H. G. 1976, *Second Reference Catalogue of Bright Galaxies* (University of Texas Press, Austin)
 de Vaucouleurs, G., de Vaucouleurs, A., Corwin, H. G., Buta, R. J., Paturel, G., & Fouque, P. 1991, *Third Reference Catalogue of Bright Galaxies* (Springer, New York)
 Disney, M., Davies, J., & Phillips, S. 1989, *MNRAS*, 239, 939
 Dressler, A. 1980, *ApJ*, 236, 51
 Efstathiou, G., Ellis, R. S., & Peterson, B. A. 1988, *MNRAS*, 232, 431
 Felten, J. 1977, *AJ*, 82, 861
 Ferguson, H. C. 1992, *Physics of Nearby Galaxies: Nature or Nurture?*, edited by T. X. Thuan, C. Balkowski, and J. Thanh Van (Editions Frontieres, Paris)
 Ferguson, H. C., & Sandage, A. 1991, *ApJ*, 101, 765
 Fukugita, M., Takahara, F., Yamashita, K., & Yoshi, Y. 1990, *ApJ*, 361, L1
 Hubble, E. 1926, *ApJ*, 64, 321
 Huchra, J. P. 1977, *ApJS*, 35, 171
 Huchra, J. P., Davis, M., Latham, D., & Tonry, J. 1983, *ApJS*, 52, 89
 Huchra, J. P., deLapparent, V., Geller, M. J. & Corwin, H. G. 1990, *ApJS*, 72, 433
 Ichikawa, T., & Fukugita, M. 1992, *ApJ*, 394, 61
 Kent, S. M. 1985, *ApJS*, 59, 115
 Kirshner, R. P., Oemler, A., & Schechter, P. L. 1979, *AJ*, 84, 951
 Koo, D. C. 1986, *ApJ*, 311, 651
 Koo, D. C., & Kron, R. G. 1992, *ARA&A*, 30, 613
 Koo, D. C., Gronwall, C., & Bruzual, G. A. 1993, *ApJL* (in press) (KGB)

- Kormendy, J. 1985, *ApJ*, 295, 73
Lacey, C., Guideroni, B., Rocca-Volmerange, B., & Silk, J. 1993, *ApJ*, 402, 15
Lauberts, A., & Valentijn, E. A. 1989, *The Surface Photometry Catalogue of the ESO-Uppsala Galaxies* (European Southern Observatory, Garching)
Loveday, J., Peterson, B. A., Efstathiou, G., & Maddox, S. J. 1992, *ApJ*, 390, 338
Marzke, R. O., Huchra, J. P., & Geller, M. J. 1993a, *ApJ* (submitted)
Marzke, R. O., daCosta, L. N., & Geller, M. J. 1993b, in preparation
Metcalf, N., Shanks, T., Fong, R., & Jones, L. R. 1991, *MNRAS*, 249, 498
Nilson, 1973, *Uppsala General Catalogue of Galaxies*, Uppsala Astr. Obs. Ann. Vol. 6
Pence, W. 1976, *ApJ*, 203, 39
Postman, M., & Geller, M. J. 1984, *ApJ*, 281, 95
Sandage, A. 1961, *Hubble Atlas of Galaxies* (Carnegie Institution of Washington, Washington), Pub. 618
Sandage, A., & Tammann, G. 1975, *ApJ*, 196, 313
Sandage, A., Tammann, G. A., & Yahil, A. 1979, *ApJ*, 232, 352
Sandage, A., & Tammann, G. A. 1981 *A Revised Shapley-Ames Catalog of Bright Galaxies* (Carnegie Institution of Washington, Washington)
Sandage, A., Binggeli, B., & Tammann, G. A. 1985, *AJ*, 90, 1759
Santiago, B. X., & Strauss M. A. 1992, *ApJ*, 387, 9
Schaeffer, R., & Silk, J. 1988, *A&A*, 203, 273
Schechter, P. 1980, *AJ*, 85, 801
Schechter, P. 1976, *ApJ*, 203, 297
Tammann, G. A., Yahil, A., & Sandage, A. 1979, *ApJ*, 234, 775
Tyson, J. A. 1988, *AJ*, 96, 1
Tyson, J. A., Valdes, F., & Wenk, R. A. 1990, *ApJ*, 349, L1
Valentijn, E. A. 1990, *Nature*, 346, 153
Vogeley, M. S., Park, C., Geller, M. J., & Huchra, J. P. 1992, *ApJ*, 391, L5
White, S. D. M., & Frenk, C. S. 1991, *ApJ*, 379, 52
Wirth, A., & Gallagher, J. S. 1984, *ApJ*, 282, 85
Yahil, A., Strauss, M. A., Davis, M., & Huchra, J. P. 1991, *ApJ*, 372, 380
Zwicky, F. Herzog, E., Wild, P., Karpowicz, M., & Kowal, C. 1961–1968, *Catalogue of Galaxies and of Clusters of Galaxies* (California Institute of Technology, Pasadena)